

# Nuclear astrophysics activities at the n\_TOF facility at CERN

Cristian Massimi<sup>1,2,\*</sup> and The n\_TOF Collaboration<sup>3</sup>

<sup>1</sup>Department of Physics and Astronomy, University di Bologna, Bologna, Italy.

<sup>2</sup>Istituto Nazionale di Fisica Nucleare (INFN), Division of Bologna, Bologna, Italy

<sup>3</sup>[www.cern.ch/ntof](http://www.cern.ch/ntof)

**Abstract.** The n\_TOF facility at CERN is operational since 2001, and provides neutron-induced cross section data of interest to several research fields, including nuclear astrophysics. The neutron time-of-flight (TOF) facility features three experimental areas located at different distances from the pulsed neutron source. Two beam lines at nominal distance of 185 and 19 m are especially equipped for TOF experiments. A third station at approximately 3 meters from the neutron source was conceived for irradiation and activation measurements. So far, neutron-induced cross sections for more than 100 isotopes have been measured.

## 1 Introduction

Radiative neutron capture, i.e.  $(n,\gamma)$ , cross sections represent one of the most relevant nuclear inputs to models of stellar nucleosynthesis of the elements heavier than iron. For instance, the  $s$  process [1, 2] proceeds via a sequence of neutron captures and  $\beta$ -decays from a distribution of seed nuclei around iron, thus building up elements up to bismuth. In this scenario,  $\beta$ -decay rates are faster than neutron capture rates, the nuclear reactions proceed along the valley of stability on the chart of nuclei.

In addition to  $(n,\gamma)$  reactions, and to a minor extent,  $(n,p)$  and  $(n,\alpha)$  reactions on a few light elements can play a relevant role when these reactions absorb a large number of neutrons, thus affecting the efficiency of the  $s$  process in synthesizing heavy elements. On the other hand,  $(n,p)$  and  $(n,\alpha)$  are of some relevance in the modelling of the nucleosynthesis occurred during Big Bang or for the study of particular topics as the stellar production of the  $^{26}\text{Al}$  gamma ray emitter observed in our galaxy.

The experimental observable of interest is the neutron-induced cross section averaged over the stellar neutron-energy distribution, typically referred to as Maxwellian averaged cross section (MACS). Experimentally, MACS are determined via two techniques: either time-of-flight (TOF) or activation. The TOF technique is based on the measurement of energy-dependent cross sections over a wide energy region, and subsequent calculation of the MCAS at different  $kT$  ( $k$  being the Boltzman constant and  $T$  the temperature). The second technique involves a sample first being irradiated with a neutron beam with a Maxwellian-like energy distribution, and subsequently the resulting product nucleus is counted. While from

---

\*e-mail: [massimi@bo.infn.it](mailto:massimi@bo.infn.it)

TOF measurements MACS between  $kT = 5$  and 100 keV can be estimated, the activation experiments are performed at a single temperature, typically around  $kT = 30$  keV.

So far, the n\_TOF collaboration has provided nuclear data using the TOF method for a large number of intriguing physics cases (see for instance ref. [3] and references therein). In the near future, the effort will be on activation measurements as well.

## 2 From laboratory experiments to stellar reaction rates

The astrophysical reaction rate depends on the number density of interacting particles times the reaction rate per particle pair  $\langle\sigma v\rangle$ . This latter term describes the probability of nuclear reactions between two particles, moving at relative velocity  $v$ . It is important to note that the interacting particles are in thermodynamic equilibrium in a stellar plasma, therefore their kinetic energy is linked to their thermal motion. Consequently as already mentioned, the relative velocity can be described by a Maxwell-Boltzmann distribution  $\phi_{MB}$ :

$$\phi_{MB}(v)dv = \phi_{MB}(E)dE = \frac{2}{\sqrt{\pi}} \frac{1}{(kT)^{3/2}} \sqrt{E} e^{-\frac{E}{kT}} dE \quad (1)$$

Figure 1 shows examples of Maxwell-Boltzmann energy distributions of neutrons in stars of different temperatures and the  $^{25}\text{Mg}(n,\gamma)$  cross section for comparison.

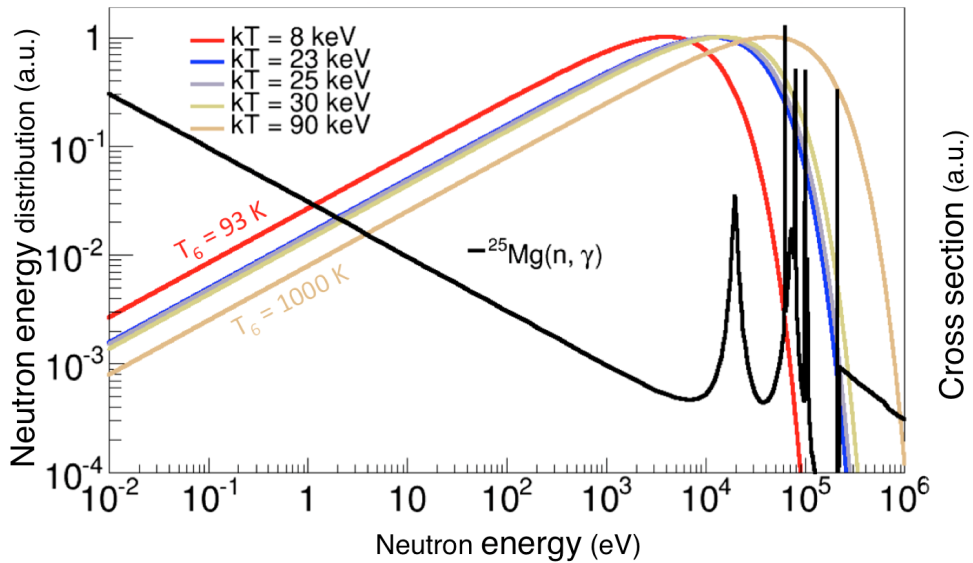


**Figure 1.** Example of energy distributions of neutrons in stellar interiors for different temperatures (colored curves), together with a  $(n,\gamma)$  cross section (black curve). For the sake of representation,  $y$ -scales are arbitrarily chosen.

From the same figure, it is evident that  $\phi_{MB}$  presents a maximum located at different energy depending on the temperature. More in detail, the maximum occurs at the velocity  $v_T = \sqrt{\frac{2kT}{\mu}}$ ,  $\mu$  being the reduced mass of the system formed by the interacting particles. As neutron-induced reaction cross sections are measured as a function of energy  $E$  (here  $E$

represents the centre-of-mass energy), it is customary to express the velocity distribution as energy distribution:

$$\langle \sigma v \rangle = \left( \frac{8}{\pi \mu} \right)^{1/2} \frac{1}{(kT)^{3/2}} \int_0^{\infty} E \sigma(E) e^{-\frac{E}{kT}} dE. \quad (2)$$

Therefore, the reaction rate can be also expressed in terms of the MACS:

$$\text{MACS} = \frac{\langle \sigma v \rangle}{v_T} = \frac{2}{\sqrt{\pi} (kT)^2} \int_0^{\infty} E \sigma(E) e^{-\frac{E}{kT}} dE. \quad (3)$$

The advantage of the TOF method with respect to activation is evident: numerical integration (Eq. 3) of energy-dependent cross section data makes it possible to derive MACSs at all relevant stellar temperatures ( $5 < kT < 100$  keV). It is important to remark that the  $\sigma(E)$  are measured over a large energy interval.

On the other hand, in case of rare and/or short-lived isotopes, it is not possible to prepare samples with sufficient mass (mg or higher) and/or enrichment for a TOF measurement. In these cases, an alternative to TOF measurements is the activation method, provided that neutron captures result in unstable isotopes. For instance, activation measurements on elements with half-life of minutes or less can be performed by cycling between irradiation and radiation measurement.

### 3 The n\_TOF facility

After several facility upgrades, now n\_TOF features two beam lines and corresponding experimental areas: EAR1 at 185 m and EAR2 at 19 m for TOF measurements, and an irradiation station referred to as NEAR for activation measurements.

The n\_TOF facility is a white spallation source driven by the CERN proton synchrotron (PS). More in particular, neutrons are produced by 20 GeV/c protons from the PS, impinging onto a massive  $80 \times 80 \times 60$  cm<sup>3</sup> Pb block [4]. The initially fast neutrons are moderated by a water layer of 5 cm, resulting in a wide neutron energy spectrum at both experimental areas EAR1 and EAR2 [5, 6]. Neutron energies span over 11 energy decades, from meV to GeV, and  $\approx 5 \times 10^5$  and  $10^7$  neutrons per bunch reach EAR1 and EAR2, respectively. Finally, some 100 times higher neutron flux with respect to EAR2 is expected at NEAR. The high instantaneous neutron flux at relative large distances from the spallation target is the result of the combination of the PS features and the ones of the neutron-producing target.

#### 3.1 Measurements at EAR1 and EAR2

The TOF technique is based on a measurement of the time needed by a neutron to travel a given distance  $L$ . This time  $t$  can be used to determine the neutron velocity:  $v = L/t$ , and consequently its kinetic energy  $E_n$ :

$$E_n = mc^2(\gamma - 1), \quad (4)$$

where  $\gamma$  represents the relativistic Lorentz factor  $\gamma = (1 - v^2/c^2)^{-1/2}$ ,  $m$  is the mass of the neutron and  $c$  is the speed of light.

The PS provides a pulsed proton beam of approximately  $10^{13}$  protons grouped in bursts of 7-ns FWHM. The primary proton beam produces a large amount of secondary particles, including  $\gamma$ -rays. These latter particles travelling along the beam pipe reach the experimental Areas after a fixed time  $t_\gamma = L/c$ , therefore providing a reference time to determine the "start" signal, i.e the moment when neutrons are produced in the spallation target. The "stop"

signal is obtained from the time of detection of the neutron-induced reaction products. Consequently, the measured TOF is obtained from the time difference between stop and start signals.

In addition to the neutron flux, a discriminating feature of neutron facilities is the energy resolution:

$$\frac{\Delta E_n}{E_n} = \gamma(\gamma + 1) \sqrt{\left(\frac{\Delta L}{L}\right)^2 + \left(\frac{\Delta t}{t}\right)^2}, \quad (5)$$

where the resolution broadening is dominated by the neutron transport in the target-moderator assembly. Thanks to the long flight paths of EAR1 and EAR2,  $\Delta E_n/E_n$  can be as small as  $10^{-4}$ .

### 3.2 Measurements at NEAR

Being so close to the neutron-producing target, NEAR is characterized by a very high neutron flux, well suited for activation measurements of astrophysical interest. The neutron beam is transported from the spallation target to the NEAR station through a collimated pipe in the shielding wall, where samples are irradiated with  $\approx 10^8$  neutrons per bunch.

This new area is complemented with a  $\gamma$ -ray spectroscopy laboratory equipped with an n-type HPGe detector of 55% relative efficiency, for the measurement of the activity resulting from irradiation of samples in the NEAR station.

Feasibility studies are ongoing to demonstrate the possibility of producing Maxwellian-like neutron spectra at different stellar temperatures by means of a neutron moderator/filter assembly, see for instance ref. [7].

In summary, after shaping the neutron spectrum to resemble a Maxwellian spectrum at a given temperature  $\phi_{MB}(kT)$ , a sample is irradiated for a certain period. The number of freshly produced nuclei are finally measured through the activity of the sample, which in first approximation is proportional to the MACS [8].

## 4 Nuclear Astrophysics at n\_TOF

So far, the n\_TOF collaboration has broadly studied different aspects of the *s*-process nucleosynthesis: (i) the main neutron sources in Red Giants stars (e.g. [9–12]); (ii) The seeds nuclei for the *s*-process (e.g. [13]); (iii) isotopes with a closed shell configuration (e.g. [14]); (iv) isotopes whose production is entirely ascribed to the *s* process (e.g. [15]); unstable isotopes where  $\beta$  decay competes with neutron capture (e.g. [16, 17]); (v) neutron poisons (e.g. [18, 19]); (vi) other reactions of interest, e.g. to Re/Os Cosmochronometer, to neutron standard [20].

Moreover, the n\_TOF collaboration promoted a program of measurements aimed at studying neutron induced charged particle reactions of astrophysical interest, amongst them the measurement of  ${}^7\text{Be}(n,\alpha)$  and  ${}^7\text{Be}(n,p)$  reactions relevant for Big Bang nucleosynthesis [21, 22], and neutron destruction of the cosmic gamma ray emitter  ${}^{26}\text{Al}$  by (n,p) and (n, $\alpha$ ) reactions [18, 19].

## References

- [1] E.M. Burbidge, G.R. Burbidge, W.A. Fowler, F. Hoyle, *Reviews of Modern Physics* **29**, 547 (1957)
- [2] F. Käppeler, R. Gallino, S. Bisterzo, W. Aoki, *Rev. Mod. Phys.* **83**, 157 (2011)

- [3] C. Massimi, S. Cristallo, C. Domingo-Pardo, C. Lederer-Woods, *Universe* **8** (2022)
- [4] R. Esposito, M. Calviani, O. Aberle, M. Barbagallo, D. Cano-Ott, T. Coiffet, N. Colonna, C. Domingo-Pardo, F. Dragoni, R. Franqueira Ximenes et al., *Physical Review Accelerators and Beams* **24**, 093001 (2021), 2106.11242
- [5] M. Barbagallo, C. Guerrero, A. Tsinganis, D. Tarrío, S. Altstadt, S. Andriamonje, J. Andrzejewski, L. Audouin, V. Bécaries, F. Bečvář et al., *European Physical Journal A* **49**, 156 (2013)
- [6] M. Sabaté-Gilarte, M. Barbagallo, N. Colonna, F. Gunsing, P. Žugec, V. Vlachoudis, Y.H. Chen, A. Stamatopoulos, J. Lerendegui-Marco, M.A. Cortés-Giraldo et al., *European Physical Journal A* **53**, 210 (2017)
- [7] G. Gervino, O. Aberle, A.P. Bernardes, N. Colonna, S. Cristallo, M. Diakaki, S. Fiore, A. Manna, C. Massimi, P. Mastinu et al., *Universe* **8** (2022)
- [8] R. Reifarth, P. Erbacher, S. Fiebiger, K. Göbel, T. Heftrich, M. Heil, F. Käppeler, N. Klapper, D. Kurtulgil, C. Langer et al., *European Physical Journal Plus* **133**, 424 (2018), 1902.09838
- [9] S. Cristallo, M. La Cognata, C. Massimi, A. Best, S. Palmerini, O. Straniero, O. Trippe, M. Busso, G.F. Ciani, F. Mingrone et al., *The Astrophysical Journal* **859**, 105 (2018), 1804.10751
- [10] P. Adsley, U. Battino, A. Best, A. Cacioli, A. Guglielmetti, G. Imbriani, H. Jayatissa, M. La Cognata, L. Lamia, E. Masha et al., *Physical Review C* **103**, 015805 (2021), 2005.14482
- [11] C. Massimi, P. Koehler, S. Bisterzo, N. Colonna, R. Gallino, F. Gunsing, F. Käppeler, G. Lorusso, A. Mengoni, M. Pignatari et al., *Physical Review C* **85**, 044615 (2012)
- [12] C. Massimi, S. Altstadt, J. Andrzejewski, L. Audouin, M. Barbagallo, V. Bécaries, F. Bečvář, F. Belloni, E. Berthoumieux, J. Billowes et al., *Physics Letters B* **768**, 1 (2017)
- [13] C. Lederer, C. Massimi, E. Berthoumieux, N. Colonna, R. Dressler, C. Guerrero, F. Gunsing, F. Käppeler, N. Kivel, M. Pignatari et al., *Physical Review C* **89**, 025810 (2014), 1403.4778
- [14] G. Tagliente, K. Fujii, P.M. Milazzo, C. Moreau, G. Aerts, U. Abbondanno, H. Álvarez, F. Alvarez-Velarde, S. Andriamonje, J. Andrzejewski et al. (n\_TOF Collaboration), *Phys. Rev. C* **77**, 035802 (2008)
- [15] A. Mazzone, S. Cristallo, O. Aberle, G. Alaerts, V. Alcayne, S. Amaducci, J. Andrzejewski, L. Audouin, V. Babiano-Suarez, M. Bacak et al., *Physics Letters B* **804**, 135405 (2020), 2002.02322
- [16] C. Lederer, C. Massimi, S. Altstadt, J. Andrzejewski, L. Audouin, M. Barbagallo, V. Bécaries, F. Bečvář, F. Belloni, E. Berthoumieux et al., *Physical Review Letters* **110**, 022501 (2013), 1304.3310
- [17] C. Guerrero, J. Lerendegui-Marco, M. Paul, M. Tessler, S. Heinitz, C. Domingo-Pardo, S. Cristallo, R. Dressler, S. Halfon, N. Kivel et al., *Physical Review Letters* **125**, 142701 (2020)
- [18] C. Lederer-Woods, P.J. Woods, T. Davinson, D. Kahl, S.J. Lonsdale, O. Aberle, S. Amaducci, J. Andrzejewski, L. Audouin, M. Bacak et al. (n\_TOF Collaboration), *Phys. Rev. C* **104**, L022803 (2021)
- [19] C. Lederer-Woods, P.J. Woods, T. Davinson, A. Estrade, J. Heyse, D. Kahl, S.J. Lonsdale, C. Paradela, P. Schillebeeckx, O. Aberle et al. (n\_TOF Collaboration), *Phys. Rev. C* **104**, L032803 (2021)

- [20] C. Massimi, C. Domingo-Pardo, G. Vannini, L. Audouin, C. Guerrero, U. Abbondanno, G. Aerts, H. Álvarez, F. Álvarez-Velarde, S. Andriamonje et al., *Physical Review C* **81**, 044616 (2010)
- [21] M. Barbagallo, A. Musumarra, L. Cosentino, E. Maugeri, S. Heinitz, A. Mengoni, R. Dressler, D. Schumann, F. Käppeler, N. Colonna et al. (n\_TOF Collaboration), *Phys. Rev. Lett.* **117**, 152701 (2016)
- [22] L. Damone, M. Barbagallo, M. Mastromarco, A. Mengoni, L. Cosentino, E. Maugeri, S. Heinitz, D. Schumann, R. Dressler, F. Käppeler et al. (The n\_TOF Collaboration [www.cern.ch/ntof]), *Phys. Rev. Lett.* **121**, 042701 (2018)